Supporting Information

A Multidimensional Nanostructural Design towards Electrochemically Stable and Mechanically Strong Hydrogel Electrodes

Wei Zhang, ·†* Jing Ma,† Wenjuan Zhang, Peigen Zhang, Wei He, Jian Chen, ZhengMing Sun*

· Prof. W. Zhang, J. Ma, Prof. P. G. Zhang, Prof. W. He, Prof. Z. M. Sun
· Jiangsu Key Laboratory of Advanced Metallic Materials
· School of Materials Science and Engineering
Southeast University, Nanjing, 211189, PR China
E-mail: w69zhang@seu.edu.cn; zmsun@seu.edu.cn
Prof. W. J. Zhang
State Key Laboratory for Advanced Processing and Recycling of Non-ferrous Metals
Lanzhou University of Technology, Lanzhou, 730050, PR China

Part 1. Calculation

Mechanical Test

The stress (σ) (MPa), strain (ε) (100%), elastic modulus (*E*) (MPa) and deformation energy (W) (MJ m^{-3}) of all MXene-based hydrogels were calculated according to eqs 1,2,3 and 4:

$$\sigma = \frac{P}{A} (1)$$

$$\varepsilon = \frac{\Delta L}{L} \times 100 (2)$$

$$E = \frac{\sigma}{\varepsilon} (3)$$

$$W = \int_0^{\varepsilon} \sigma d\varepsilon (4)$$

where *P* (N) is the maximum load along the direction of applied force at fracture, *A* (mm^2) is the cross-sectional area of the fracture. ΔL is breaking elongation and *L* is the original length.

Electrochemical Characterization

The electrochemical performances of all MXene-based hydrogel electrodes were performed in a three-electrode system. The work electrode was MXene-based hydrogels (size of 10 mm × 10 mm × 2 mm), the reference electrode was Hg/Hg_2SO_4 electrode (Shanghai Lei Magnetism Instrument Co., Ltd.), and the counter electrode was a titanium plate, respectively.

The specific capacitance (C_p) ($F \cdot g^{-1}$) of all electrodes were calculated according to their GCD curves and derived from eq 5:

$$C_p = \frac{I \times \Delta t}{m \times \Delta V} (5)$$

where I is the discharge current, Δt is the discharge time of CGD curves, m is the mass of active materials in single working electrodes, and ΔV is the voltage change during discharge.

For flexible symmetric solid-state supercapacitors, the electrochemical performance were measured in a two electrode system. The cell-specific capacitance (C_{cell}) ($F \cdot g^{-1}$) of all solid-state supercapacitor devices were calculated from their CGD curves according to eq 6:

$$C_{cell} = \frac{I \times \Delta t}{M \times \Delta V} (6)$$

where *I* is the discharge current, Δt is the discharge time of CGD curves, *m* is the mass of active materials in two pieces working electrodes, and ΔV is the voltage change during discharge.

The energy density (E_{cell}) and power density (P_{cell}) of the supercapacitor devices were calculated based on eqs 7 and 8:

$$E_{cell} = \frac{C_{cell} \times (\Delta V)^2}{2 \times 3.6} (7)$$

$$P_{cell} = \frac{E_{cell} \times 3600}{\Delta t} \quad (8)$$

where E_{cell} is the energy density, P_{cell} is the power density and C_{cell} is the cell- specific capacitance, the ΔV is the voltage change during discharge, the Δt is the discharge time from GCD curves.

Part 2. Figures

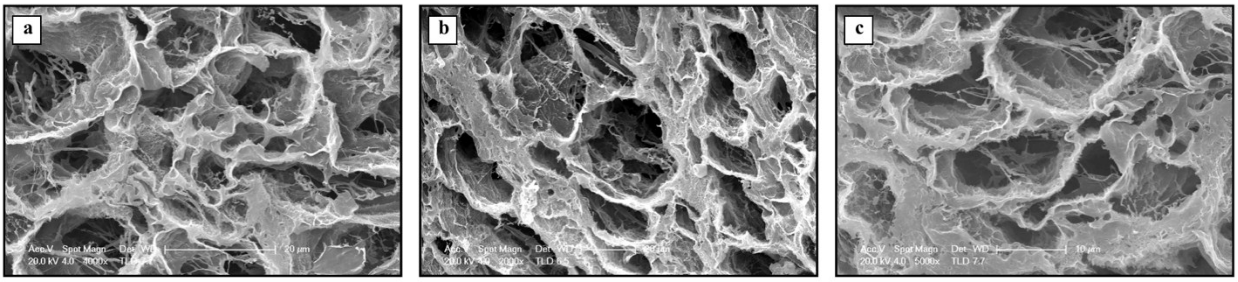

Figure S1: SEM images of MXene-PVA hydrogels with different MXene concentrations: (a) 0.2 mg cm^{-3}; (b) 0.4 mg cm^{-3}; and (c) 2.0 mg cm^{-3}.

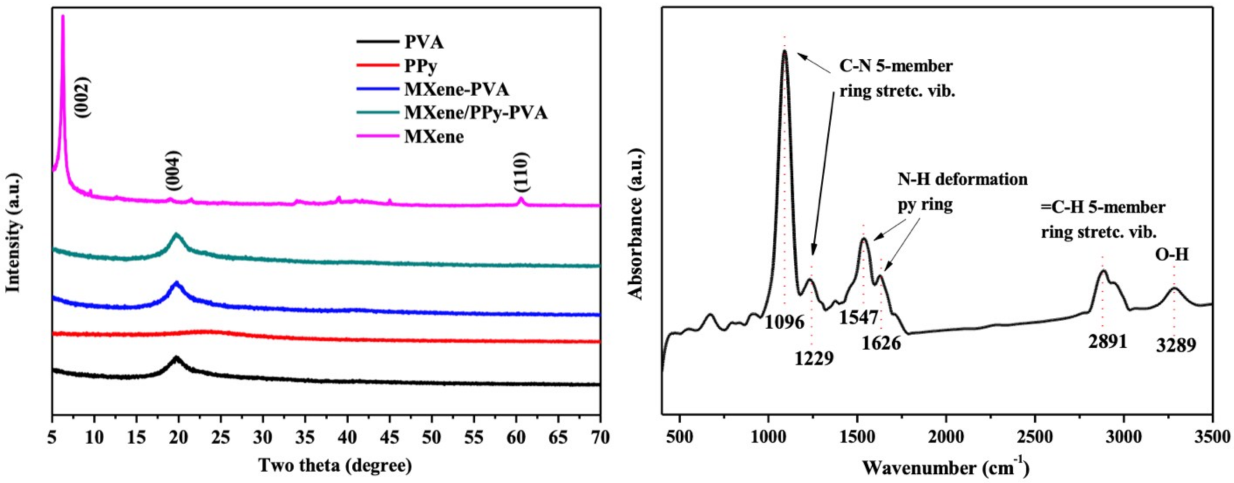

Figure S2. (a) XRD patterns of the PVA, PPy, MXene-PVA, MXene/PPy-PVA and MXene; (b) FTIR spectrum of the MXene/PPy-PVA hydrogel.

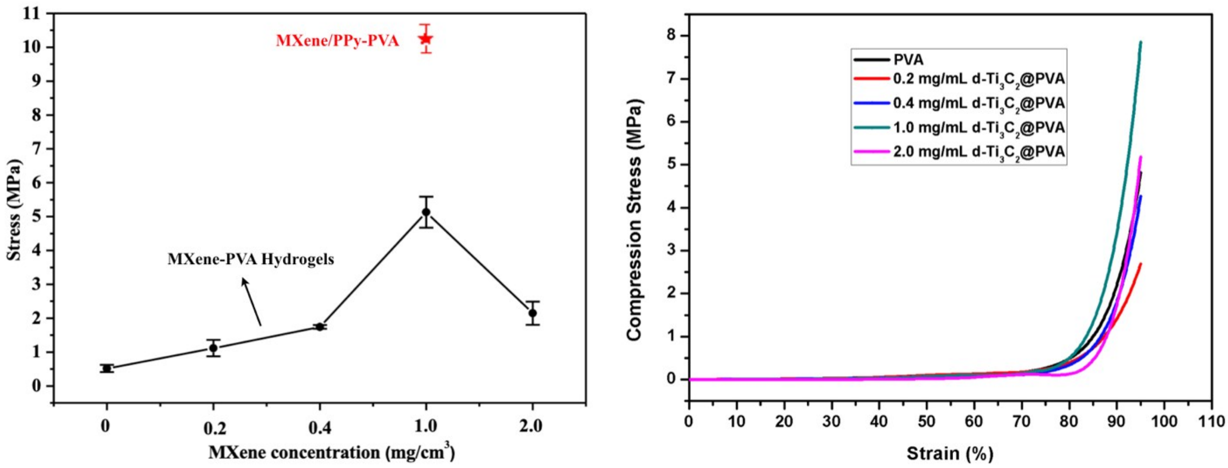

Figure S3. (a) The Maximum tensile stress of MXene-PVA hydrogels with different MXene concentrations, (b) Compression stress-strain curves of PVA and different concentration MXene-PVA hydrogels

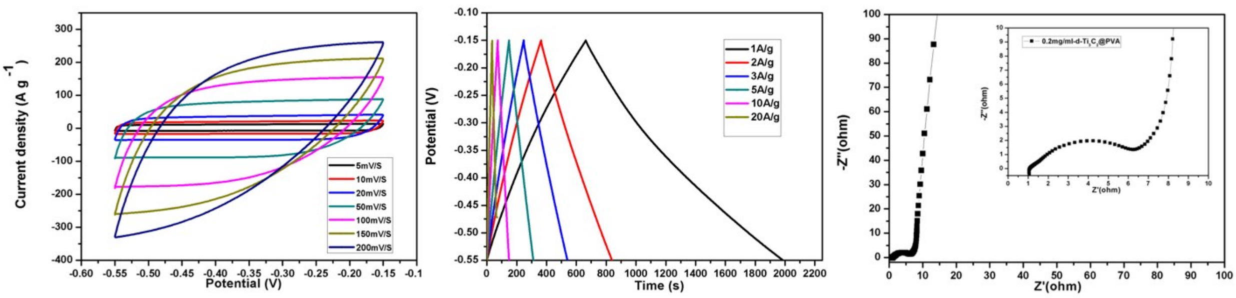

Figure S4. Electrochemical characterizations of 0.2 mg cm^{-3} MXene hydrogel electrodes: (a) CV, (b) charge/ discharge, and (c) EIS curves.

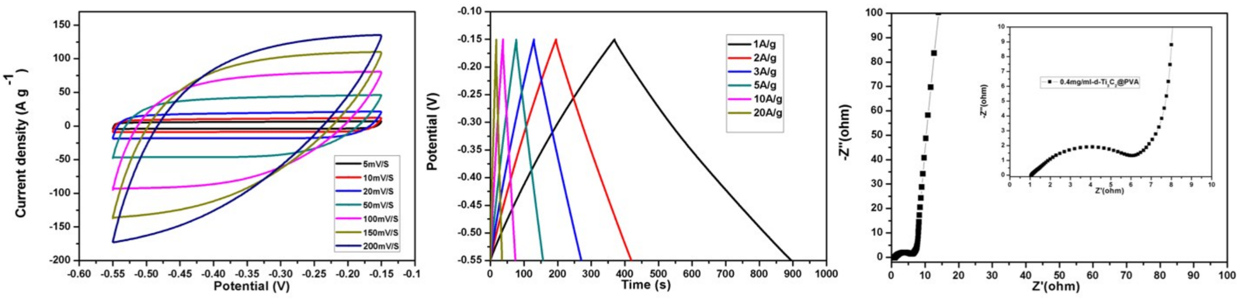

Figure S5. Electrochemical characterizations of 0.4 mg cm^{-3} MXene hydrogel electrodes: (a) CV, (b) charge/ discharge, and (c) EIS curves.

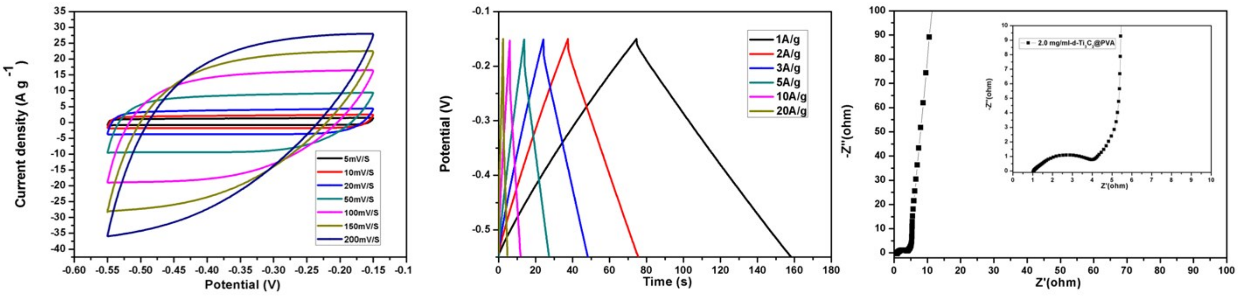

Figure S6. Electrochemical characterizations of 2 mg cm^{-3} MXene hydrogel electrodes: (a) CV, (b) charge/ discharge, and (c) EIS curves.

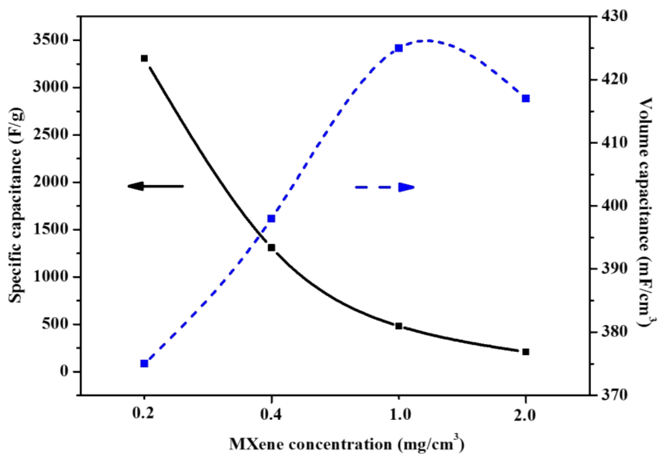

Figure S7. Specific capacitance and volume capacitance of MXene-PVA electrodes with different MXene concentration.

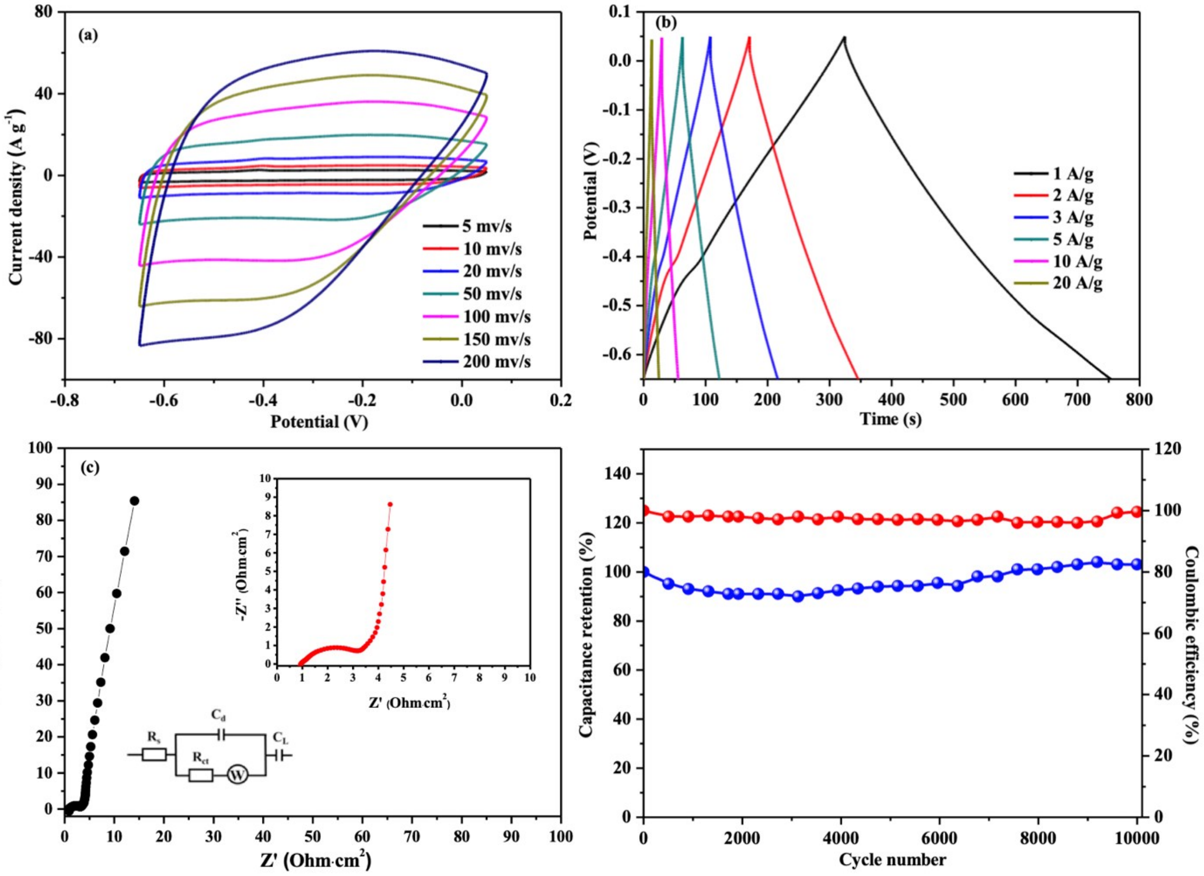

Figure S8. Electrochemical characterizations of MXene/PPy-PVA hydrogel electrodes: (a) CV, (b) charge/ discharge, (c) EIS curves, and (d) The cycle life and coulombic efficiency.

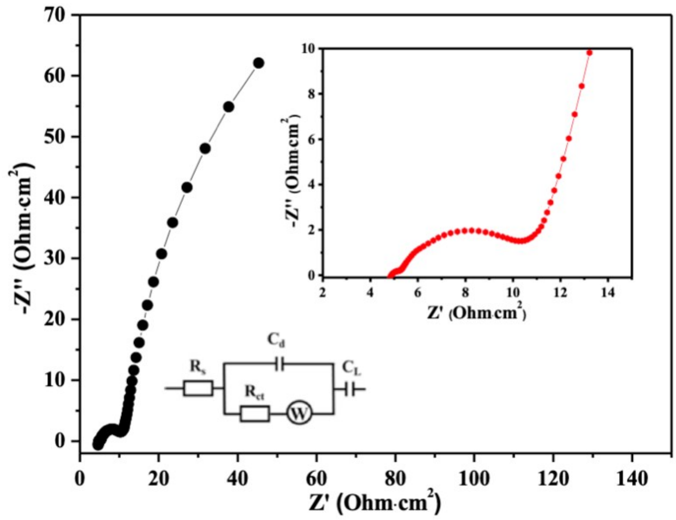

Figure S9. EIS curves of the assembled flexible supercapacitor.

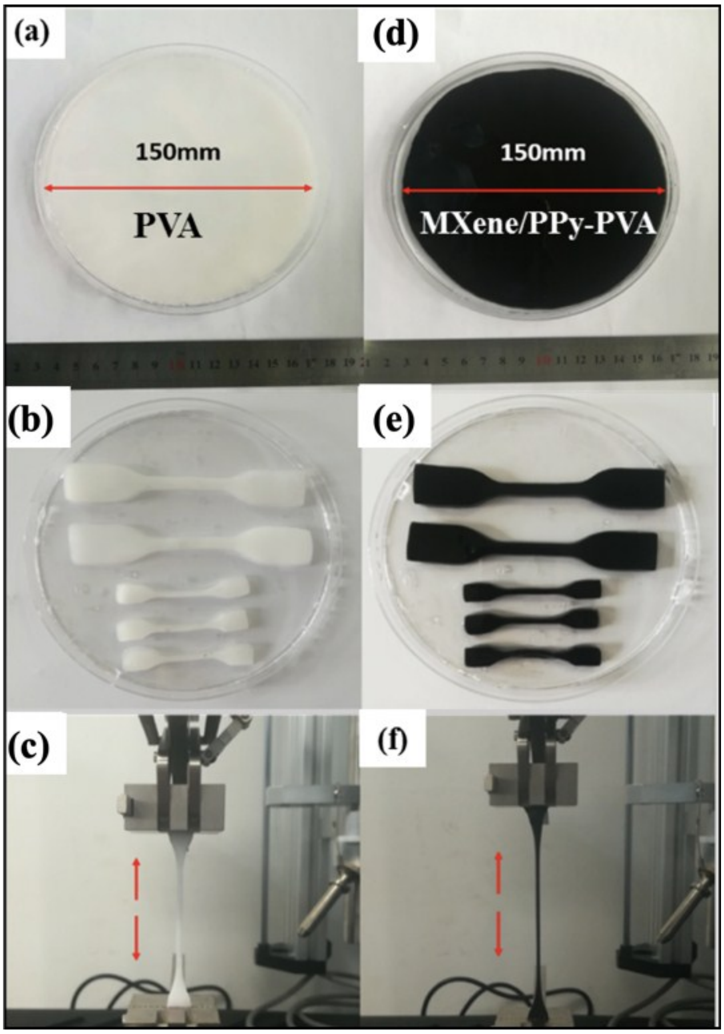

Figure S10. Photographs of PVA and MXene/PPy-PVA hydrogels durying tensile tests: (a), (b) and (c) were PVA hydrogels; (d), (e) and (f) were MXene/PPy-PVA hydrogels.

Part 3. Tables

Table S1. Mass specific capacitance and tensile strength of different hydrogel electrode materials

Hydrogel electrodes	Specific capacitance (F g^{-1})	Tensile strength (MPa)	Ref.
PANI@CNF-PVA	201.6 at 1 A g^{-1}	0.032	1
PVAB@CNT-CNF	117.1 at 1 A g^{-1}	0.093	2
PANI	750 at 1 A g^{-1}	0.600	3
Polythiophene	135 at 1 A g^{-1}	160	4
PANI@CNT_S@PLA	510.3 at 1 A g^{-1}	18.7	5
CTS@SA	234.6 at 1 A g^{-1}	0.290	6
PANI@GO	115.2 at 1 A g^{-1}	351.9	7
Graphene	175 at 1 A g^{-1}	0.450	8
MXene@PPy-PVA	614 at 1 A g^{-1}	10.3	our work

Part 4. Movies

For the movies, Movie S1 and S2 show the stretching properties of pure PVA and MXene-PVA hydrogel cylinders. The pure PVA hydrogel can be broken easily, while the MXene-PVA shows strong mechanical strength. Movie S3 and S4 show the cyclic compression of pure PVA and MXene-PVA hydrogel cylinders. The pure PVA hydrogel can be broken easily, while the MXene-PVA shows strong compression strength.

References

[1] J. Han, Q. Ding, C. Mei, Q. Wu, Y. Yue, X. Xu, *Electrochimica Acta* **2019**, *318*, 660.

[2] J. Han, H. Wang, Y. Yue, C. Mei, J. Chen, C. Huang, Q. Wu, X. Xu, *Carbon* **2019**, *149*, 1.

[3] H. Guo, W. He, Y. Lu, X. Zhang, *Carbon* **2015**, *92*, 133.

[4] Q. Chen, X. Wang, F. Chen, N. Zhang, M. Ma, *Chem. Eng. J.* **2019**, *368*, 933.

[5] Q. Wang, H. Wang, P. Du, J. Liu, D. Liu, P. Liu, *Electrochimica Acta* **2019**, *294*. 312.

[6] J. Zhao, Y. Chen, Y. Yao, Z.-R. Tong, P.-W. Li, Z.-M. Yang, S.-H. Jin, *J. Power Sources* **2018**, *378*, 603.

[7] C. Wu, T. Zhou, Y Du, S. Dou, H. Zhang, L. Jiang, Q. Cheng, *Nano Energy* **2019**, *58*, 517.

[8] Y. Xu, K. Sheng, C. Li, G. Shi, *ACS Nano* **2010**, *4*, 4324.